

Mixed-Metal Cluster Chemistry. 30.¹ Syntheses and Optical Limiting Properties of Cluster-Containing Oligo- and Polyurethanes

Michael D. Randles,[†] Nigel T. Lucas,[†] Marie P. Cifuentes,[†] Mark G. Humphrey,^{*,†} Matthew K. Smith,[‡] Anthony C. Willis,[‡] and Marek Samoc[§]

Department of Chemistry, Australian National University, Canberra, ACT 0200, Australia, Research School of Chemistry, Australian National University, Canberra, ACT 0200, Australia, and Laser Physics Centre, Research School of Physical Sciences and Engineering, Australian National University, Canberra, ACT 0200, Australia

Received May 10, 2007; Revised Manuscript Received August 16, 2007

ABSTRACT: Molybdenum–iridium clusters $\text{Mo}_2\text{Ir}_2\{\mu_4\text{-}\eta^2\text{-C}_2[(\text{CH}_2)_6\text{OH}]_2\}(\mu\text{-CO})_4(\text{CO})_4(\eta\text{-C}_5\text{H}_4\text{R})_2$ [$\text{R} = \text{H}$ (**5**), Me (**6**), $(\text{CH}_2)_9\text{O(THP)}$ (**7**); THP = tetrahydropyranyl] are formed from reaction of $\text{Mo}_2\text{Ir}_2(\mu\text{-CO})_3(\text{CO})_7(\eta\text{-C}_5\text{H}_4\text{R})_2$ with the alkyne $\text{HO}(\text{CH}_2)_6\text{C}_2(\text{CH}_2)_6\text{OH}$. Reaction of **6** and **7** with the diisocyanate $\text{OCN}(\text{CH}_2)_4\text{NCO}$ affords oligourethanes $[-\text{O}(\text{CH}_2)_6(\mu_4\text{-}\eta^2\text{-C}_2)\{\text{Mo}_2\text{Ir}_2(\mu\text{-CO})_4(\text{CO})_4(\eta\text{-C}_5\text{H}_4\text{R})_2\}(\text{CH}_2)_6\text{OC(O)NH}(\text{CH}_2)_4\text{NHC(O)-}]_n$ [$\text{R} = \text{Me}$ (**12**), $(\text{CH}_2)_9\text{O(THP)}$ (**13**)], with transition metal clusters in the backbone, the extent of polymerization being ascertained by size exclusion chromatography and ¹H NMR spectroscopy. Characterization of the cluster-containing oligo- and polyurethanes was aided by ¹H NMR and IR spectral comparison with model cluster diurethanes $\text{Mo}_2\text{Ir}_2\{\mu_4\text{-}\eta^2\text{-C}_2[(\text{CH}_2)_6\text{OC(O)NH}(\text{CH}_2)_3\text{Me}]_2\}(\mu\text{-CO})_4(\text{CO})_4(\eta\text{-C}_5\text{H}_4\text{R})_2$ [$\text{R} = \text{H}$ (**8**), Me (**9**), $(\text{CH}_2)_9\text{O(THP)}$ (**11**)], prepared from reaction between the cluster diols **5**, **6**, and **7** and the isocyanate $\text{Me}(\text{CH}_2)_3\text{NCO}$. The diol cluster **5** and cluster diurethane **8** have been characterized by single-crystal X-ray diffraction studies. Removal of the THP groups in **13** gives $[-\text{O}(\text{CH}_2)_6(\mu_4\text{-}\eta^2\text{-C}_2)\{\text{Mo}_2\text{Ir}_2(\mu\text{-CO})_4(\text{CO})_4(\eta\text{-C}_5\text{H}_4(\text{CH}_2)_9\text{OH})_2\}(\text{CH}_2)_6\text{OC(O)NH}(\text{CH}_2)_4\text{NHC(O)-}]_n$ (**14**), which has been cross-linked on reaction with $\text{OCN}(\text{CH}_2)_4\text{NCO}$. The cluster content of the polyurethanes can be diluted; polymerization of 1:19 **6**:1,6-hexanediol and $\text{OCN}(\text{CH}_2)_4\text{NCO}$ affords copolymer $[-\text{O}(\text{CH}_2)_6(\mu_4\text{-}\eta^2\text{-C}_2)\{\text{Mo}_2\text{Ir}_2(\mu\text{-CO})_4(\text{CO})_4(\eta\text{-C}_5\text{H}_4\text{Me})_2\}(\text{CH}_2)_6\text{OC(O)NH}(\text{CH}_2)_4\text{NHC(O)}\{\text{O}(\text{CH}_2)_6\text{OC(O)NH}(\text{CH}_2)_4\text{NHC(O)}\}_m-]_n$ (**16**). The optical limiting properties of these dimolybdenum–diiridium clusters and cluster-containing polymers, and related molybdenum–triiridium clusters and tungsten-containing homologues, have been assessed by open-aperture Z-scan studies at 527 nm employing ns pulses. Optical limiting merit increases upon increasing group 6 metal content, and replacing the 4d metal molybdenum with the 5d metal tungsten. Some insight into the mechanism by which these clusters function as optical limiters has been gleaned from complementary pump–probe studies, with their behavior consistent with a fast nonlinear absorption process followed by reverse saturable absorption involving metastable excited states of greater than nanosecond lifetime.

Introduction

There has been significant recent interest in the incorporation of transition metal atoms into polymer frameworks, because the metal may imbue the polymer with specific optical, electronic, magnetic, catalytic, and other properties. Incorporation of polymetallic “cluster” species would be expected to result in enhancement of these properties or possibly introduce fundamentally new behavior, but until recently there was a dearth of robust cluster-containing polymers—the vast majority of examples involve cluster–polymer attachment via P- or N-ligands, a readily dissociable coordination that can result in cluster-containing polymer breakdown.²

Materials with optical limiting properties are required for a variety of applications, and they are generally needed in a form suitable for preparation of films. Organometallic clusters have been identified as being among the most promising materials for optical limiting applications.³ Unfortunately, due to the rigid nature of the cluster core, and consequent easy crystallization, the processability of such clusters is a problem. Incorporating the cluster into a polymer is expected to enhance the process-

ability. As long as the cluster units are kept in a uniform environment and do not electronically interact, the optical limiting capabilities of the individual cluster units should not be affected. We have previously reported incorporation of pseudotetrahedral dimolybdenum–diiridium clusters into oligomer main chains by using 2-hydroxyethyl-functionalized cyclopentadienyl ligands, but the short two-carbon linkage detrimentally affects the extent of polymerization.⁴ We report herein studies employing ligands with longer “spacer” units, namely 9-hydroxynonyl-functionalized cyclopentadienyl and tetradec-7-yne-1,14-diol, that have afforded higher molecular weight species, together with studies assessing the optical limiting merit of these cluster-containing systems.

Experimental Section

Materials. All reactions were carried out under an atmosphere of nitrogen using standard Schlenk techniques. All glassware used in reactions involving sodium, sodium hydride or isocyanates was flame-dried under vacuum before use. All cluster complexes seemed stable in air as solids and for at least short periods of time in solution, and thus no special precautions were taken to exclude air in their manipulation. The reaction solvents THF and *p*-dioxane were distilled under nitrogen over sodium benzophenone ketyl, while CH_2Cl_2 was distilled over CaH_2 under nitrogen; all other solvents were used as received. Petroleum spirit refers to the petroleum fraction of boiling range 60–80 °C. Non-polymeric cluster compounds were purified by preparative thin-layer chromatography (TLC) on 20 × 20 cm glass plates coated with Merck

* Corresponding author. Telephone: +61 2 6125 2927. Fax: +61 2 6125 0760. E-mail: Mark.Humphrey@anu.edu.au.

[†] Department of Chemistry, Australian National University.

[‡] Research School of Chemistry, Australian National University.

[§] Laser Physics Centre, Research School of Physical Sciences and Engineering, Australian National University.

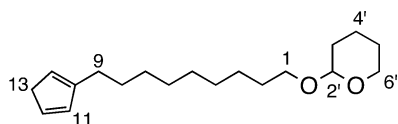


Figure 1. Numbering scheme for NMR assignments.

GF₂₅₄ silica gel (0.5 mm). Column chromatography was performed using Merck silica gel 60 of particle size 0.040–0.063 mm (230–400 mesh ASTM).

Cyclopentadiene (Aldrich) was distilled from dicyclopentadiene before use. Molybdenum hexacarbonyl, sodium metal, sodium hydride (60% dispersion in mineral oil), anhydrous potassium carbonate, butyl isocyanate, 1,4-diisocyanatobutane, and dibutyltin diacetate (Aldrich) were used as received. *n*-Butyllithium (solution in cyclohexane, Aldrich) was titrated with diphenylacetic acid in diethyl ether prior to each use to determine its exact concentration. Liquid reagents were deoxygenated by purging with nitrogen prior to addition. Literature procedures were used to synthesize IrCl(CO)₂(*p*-toluidine),⁵ MoIr₃(μ-CO)₃(CO)₈(η-C₅H₅) (18),⁶ Mo₂Ir₂(μ-CO)₃(CO)₇(η-C₅H₅)₂ (3),⁷ Mo₂Ir₂(μ-CO)₃(CO)₇(η-C₅H₄Me)₂,⁸ Mo₂Ir₂(μ-CO)₃(CO)₇(η-C₅Me₅)₂ (17),⁸ W₂Ir₂(CO)₁₀(η-C₅H₅)₂ (19),⁹ Mo₂Ir₂(μ-CO)₃(CO)₇(η-C₅H₄(CH₂)₂OC(O)NH(CH₂)₅Me)₂ (20),⁴ [-(O(CH₂)₂-η-C₅H₄)Mo₂Ir₂(μ-CO)₃(CO)₇(η-C₅H₄(CH₂)₂OC(O)NH(CH₂)₆NHC(O)-)]₅ (21),⁴ Mo₂Ir₂(μ₄-η²-MeC₂Ph)(μ-CO)₄(CO)₄(η-C₅H₄Me)₂ (22),¹⁰ 2-(9-bromononyloxy)tetrahydro-2*H*-pyran,¹¹ 2-(14-(tetrahydro-2*H*-pyran-2-yloxy)tetradec-7-ynyloxy)tetrahydro-2*H*-pyran,¹¹ and tetradec-7-yne-1,14-diol.¹¹

Instruments. Infrared spectra were recorded in AR grade CH₂Cl₂ solvent on a Perkin-Elmer System 2000 FT-IR spectrometer in a solution cell with CaF₂ windows; spectral features are reported in cm⁻¹. ¹H and ¹³C NMR spectra were recorded on a Varian Gemini-300 spectrometer (¹H at 300 MHz, ¹³C at 75 MHz). Spectra were recorded in CDCl₃ and referenced to residual solvent peaks. All ¹H NMR spectral assignments are based on the numbering scheme given in Figure 1. Electron impact (EI) mass spectra (unit resolution and high resolution) were recorded using a VG Autospec instrument. Electrospray ionization (ESI) mass spectra were recorded using either a Bruker Apex 4.7T FTICR-MS instrument or a VG Platform II mass spectrometer. Mass spectra are reported in the form: *m/z* (assignment, relative intensity). Microanalyses were carried out by the Microanalysis Service Unit in the Research School of Chemistry, ANU. Polymer molecular weights were measured using a Shimadzu GPC connected to a UV-detector at the Key Centre for Polymer Colloids, University of Sydney. Experiments were run in THF, with a flow rate of 1.0 mL min⁻¹. The system was equipped with three Styragel columns: HR4, HR3, and HR1 (with effective molecular weight ranges of 5000–500000, 500–30000, and 100–5000, respectively). The GPC was calibrated using monodisperse polystyrene standards ranging from 580 to 390000 in molecular weight. The modulated DSC of 12 was conducted on a TA Instruments DSC 2920, on a 4.7 mg sample in an anodized hermetically sealed pan, cycling between –60 and +150 °C, twice. The temperature was modulated ±1 °C per 60 s, heating at a rate of 5 °C per min.

Synthesis of 2-{9-(Cyclopenta-1,4-dienyl)nonyloxy}tetrahydro-2*H*-pyran (1). Activated sodium metal (480 mg, 20.9 mmol) was added to a solution of freshly distilled cyclopentadiene (1.00 mL, 15.1 mmol) in THF (30 mL) and the resultant mixture stirred for 6 h at room temperature. The solution was separated from the unreacted sodium by transfer via a cannula into a second Schlenk tube. The sodium cyclopentadienide solution was cooled to –78 °C, and a solution of 2-(9-bromononyloxy)tetrahydro-2*H*-pyran (2.31 g, 7.50 mmol) in THF (15 mL) was added dropwise. The solution was allowed to stand at 0 °C in the fridge for 16 h, before being filtered from the white precipitate that had settled. Diethyl ether (50 mL) was added and the ethereal solution was washed with brine (3 × 40 mL), dried over potassium carbonate and the volatile materials removed in vacuo. The crude residue was applied to a 20 cm silica column and eluted with petroleum spirits. Fractions were collected during gradient elution with petroleum spirits/CH₂-

Cl₂ mixtures. Like fractions were combined and the solvents removed under vacuum. The major band contained 2-{9-(cyclopenta-1,4-dienyl)nonyloxy}tetrahydro-2*H*-pyran (1) as a pale yellow liquid (mixture of isomers), 1.27 g (4.34 mmol, 58%). ¹H NMR: δ 6.42–5.96 (m, 3H, H11, H12 and H14), 4.56 (t, *J* = 4.4 Hz, 1H, H2'), 3.88–3.81, and 3.51–3.45 (2 × m, 2H, H6'), 3.74–3.66 and 3.39–3.31 (2 × m, 2H, CH₂O(THP)), 2.92–2.85 (m, 2H, H13), 2.38–2.30 (m, 2H, CH₂Cp), 1.89–1.47 (m, 8H), 1.27 (br s, 12H). ¹³C NMR: δ 98.9 (C2'), 67.8 (CH₂O(THP)), 62.4 (C6'), 30.8, 29.8, 29.6, 26.3, 25.6, 19.8. MS(EI): 292 ([M]⁺, 40), 207 ([M – THP]⁺, 4), 191 ([M – O(THP)]⁺, 3), 85 ([THP]⁺, 100). HR-MS (EI): calculated, C₁₉H₃₂O₂, 292.2402; found, 292.2402.

Synthesis of Mo₂Ir₂(μ-CO)₃(CO)₇(η-C₅H₄(CH₂)₂O(THP))₂ (2). Sodium hydride (226 mg as a 60% dispersion in oil, 5.66 mmol) was added to a flame-dried Schlenk tube containing 2-{9-(cyclopenta-1,4-dienyl)nonyloxy}tetrahydro-2*H*-pyran (1) (725 mg, 2.48 mmol) in THF (30 mL). The mixture was stirred at room temperature for 18 h, and then the excess sodium hydride was filtered off. An aliquot of THF (10 mL) was used to wash the sodium hydride residue. Mo(CO)₆ (697 mg, 2.64 mmol) was added, and the mixture was heated under reflux for 24 h. After cooling, the THF was removed in vacuo and IrCl(CO)₂(*p*-toluidine) (557 mg, 1.42 mmol) in CH₂Cl₂ (30 mL) was added and the mixture was stirred for 2 h at room temperature, during which time the color darkened. The solvent was removed in vacuo, and the crude residue was dissolved in the minimum amount of CH₂Cl₂ and applied to preparative silica TLC plates. Elution with CH₂Cl₂/acetone (24:1) afforded five bands. The contents of the first (*R*_f = 0.91, orange), third (*R*_f = 0.69, black), fourth (*R*_f = 0.45, yellow), and fifth (*R*_f = 0.38, pink) bands all appeared to be in trace amounts and were not isolated. The contents of the second and major band (*R*_f = 0.82, brown) were extracted with CH₂Cl₂ to afford a brown oil, identified as cluster 2 (285 mg, 0.198 mmol, 28%). IR: ν(CO, cluster) 2059 vs, 2030 vs, 2005 vs, 1983 w, 1966 sh, 1925 s, 1884 m, 1846 m, 1800 w, 1758 m cm⁻¹. ¹H NMR: δ 4.83–4.76 (m, 8H, C₅H₄R), 4.54 (t, *J*_{HH} = 4.4 Hz, 2H, H2'), 3.87–3.81 and 3.49–3.43 (2 × m, 4H, H6'), 3.74–3.66 and 3.39–3.31 (2 × m, 4H, CH₂O(THP)), 2.22 (t, *J*_{HH} = 7.1 Hz, 4H, CH₂Cp), 1.89–1.47 (m, 16H), 1.25 (br s, 24H). ¹³C NMR: δ 108.9 (C₅H₄R), 98.9 (C2'), 94.5 (C₅H₄R), 89.3 (C₅H₄R), 67.7 (CH₂O(THP)), 62.4 (C6'), 32.3, 30.8, 29.8, 29.6, 29.4, 29.3, 29.2, 26.3, 26.2, 25.6, 19.8. MS (ESI): 1461 ([M + Na]⁺, 13), 1405 ([M + Na – 2CO]⁺, 36).

Synthesis of Mo₂Ir₂{μ₄-η²-C₂[(CH₂)₆OH]₂}(μ-CO)₄(CO)₄(η-C₅H₅)₂ (5). Tetradec-7-yne-1,14-diol (98.0 mg, 0.433 mmol) was added to a red-brown solution of Mo₂Ir₂(μ-CO)₃(CO)₇(η-C₅H₅)₂ (3) (82.0 mg, 0.0831 mmol) in CH₂Cl₂ (30 mL) and the resultant mixture stirred under reflux for 24 h, over which time the color changed to dark green. The solution was taken to dryness in vacuo, and then the crude residue was dissolved in the minimum amount of CH₂Cl₂ and applied to preparative silica TLC plates. Elution with CH₂Cl₂/acetone (3:1) afforded four bands. The contents of the first (*R*_f = 0.69, green), second (*R*_f = 0.58, green), and fourth (*R*_f = 0.33, green) bands all appeared to be in trace amounts and were not isolated. The contents of the third band (*R*_f = 0.51, green) were extracted with acetone to afford a green solid, identified as the alkyne-derived diol cluster 5 (92.1 mg, 0.0796 mmol, 96%). Diffusion of *n*-hexane into a solution of 5 in CH₂Cl₂ at 4 °C gave a dark green crystal suitable for the structural study. IR: ν(CO, cluster) 2068 vs, 2040 vs, 2012 m, 1995 m, 1810 s, 1762 s cm⁻¹. ¹H NMR: δ 4.99 (s, 10H, C₅H₅), 3.62 (t, *J*_{HH} = 6.6 Hz, 4H, CH₂-OH), 2.13 (m, 4H, CH₂C₂), 1.65–1.23 (m, 16H, CH₂). ¹³C NMR (CDCl₃): δ 96.5 (C₅H₅), 80.3 (C₂), 63.0 (CH₂OH), 32.7, 29.0, 28.6, 25.3, 18.7. MS (ESI): 1193 ([M + Cl]⁺, 100), 1165 ([M + Cl – CO]⁺, 20), 1137 ([M + Cl – 2CO]⁺, 16), 1109 ([M + Cl – 3CO]⁺, 14), 1081 ([M + Cl – 4CO]⁺, 50), 1053 ([M + Cl – 5CO]⁺, 75), 1025 ([M + Cl – 6CO]⁺, 87).

Synthesis of Mo₂Ir₂{μ₄-η²-C₂[(CH₂)₆OH]₂}(μ-CO)₄(CO)₄(η-C₅H₄Me)₂ (6). Tetradec-7-yne-1,14-diol (294 mg, 1.30 mmol) was added to an orange-brown solution of Mo₂Ir₂(μ-CO)₃(CO)₇(η-C₅H₄Me)₂ (4) (306 mg, 0.302 mmol) in CH₂Cl₂ (50 mL) and the resultant mixture stirred under reflux for 24 h, over which time the color

changed to dark green. The solution was taken to dryness in vacuo, and then the crude residue was dissolved in the minimum amount of CH_2Cl_2 and applied to preparative silica TLC plates. Elution with $\text{CH}_2\text{Cl}_2/\text{acetone}$ (7:3) afforded four bands. The contents of the first (R_f = solvent line, brown), second (R_f = 0.81, green), and third (R_f = 0.66, green) bands all appeared to be in trace amounts and were not isolated. The contents of the fourth band (R_f = 0.57, green) were extracted with acetone to afford a green solid, identified as the alkyne-derived diol cluster **6** (321 mg, 0.271 mmol, 90%). IR: $\nu(\text{CO, cluster})$ 2065 vs, 2037 vs, 2009 m, 1991 m, 1809 s, 1761 s cm^{-1} . ^1H NMR: δ 4.78–4.69 (m, 8H, $\text{C}_5\text{H}_4\text{Me}$), 3.62 (t, J_{HH} = 6.6 Hz, 4H, CH_2OH), 2.13 (m, 4H, CH_2C_2), 1.61–1.23 (m, 16H, CH_2). ^{13}C NMR (CDCl_3): δ 103.6 ($\text{C}_5\text{H}_4\text{Me}$), 98.5 ($\text{C}_5\text{H}_4\text{Me}$), 95.9 ($\text{C}_5\text{H}_4\text{Me}$), 80.3 (C_2), 63.0 (CH_2OH), 32.7, 29.2, 29.0, 28.6, 26.0, 25.3, 18.7. MS (ESI): 1215 ($[\text{M} + \text{OMe}]^-$, 100), 1157 ($[\text{M} - \text{CO}]^-$, 30).

Synthesis of $\text{Mo}_2\text{Ir}_2\{\mu_4\text{-}\eta^2\text{-C}_2[(\text{CH}_2)_6\text{OH}]_2\}(\mu\text{-CO})_4(\text{CO})_4\{\eta\text{-C}_5\text{H}_4(\text{CH}_2)_9\text{O(THP)}\}_2$ (7**).** Tetradec-7-yne-1,14-diol (187 mg, 0.826 mmol) was added to a brown solution of **2** (226 mg, 0.157 mmol) in CH_2Cl_2 (50 mL), and the resultant mixture was stirred at room temperature for 48 h and then under reflux for 24 h, over which time the color changed to dark green. The solution was taken to dryness in vacuo, and then the crude residue was dissolved in the minimum amount of CH_2Cl_2 and applied to preparative silica TLC plates. Elution with $\text{CH}_2\text{Cl}_2/\text{acetone}$ (4:1) afforded four bands. The contents of the first (R_f = 1.00, brown, 79.5 mg), second (R_f = 0.84, green, 9.9 mg), and fourth (R_f = 0.40, brown, 93.9 mg) bands were all extracted with acetone, but could not be identified. The contents of the third band (R_f = 0.51, green) were extracted with acetone to afford a green oil, identified as **7** (67.6 mg, 0.0420 mmol, 27%). IR: $\nu(\text{CO})$ 2065 vs, 2037 vs, 2008 m, 1991 m, 1808 s, 1759 s cm^{-1} . ^1H NMR: δ 4.86–4.77 (m, 8H, $\text{C}_5\text{H}_4\text{R}$), 4.58–4.53 (m, 2H, H_2'), 3.88–3.81 and 3.51–3.45 (2 m, 4H, H_6'), 3.74–3.66 and 3.39–3.31 (2 m, 4H, $\text{CH}_2\text{O(THP)}$), 3.65–3.59 (m, 4H, CH_2OH), 2.29–2.23 (m, 4H, CH_2Cp), 2.14–2.09 (m, 4H, CH_2C_2), 1.68–1.22 (m, 56H, CH_2). ^{13}C NMR: δ 103.4 ($\text{C}_5\text{H}_4\text{R}$), 99.1 (C_2'), 98.4 ($\text{C}_5\text{H}_4\text{R}$), 94.7 ($\text{C}_5\text{H}_4\text{R}$), 80.2 (C_2), 67.5 (C_1), 63.1 (CH_2OH), 62.3 (C_6'), 32.8, 30.8, 29.8, 29.6, 29.5, 29.4, 29.3, 29.2, 26.9, 26.5, 25.8, 25.5, 19.9. MS (ESI): 1646 ($[\text{M} + \text{Cl}]^-$, 94), 1618 ($[\text{M} + \text{Cl} - \text{CO}]^-$, 30), 1590 ($[\text{M} + \text{Cl} - 2\text{CO}]^-$, 25), 1562 ($[\text{M} + \text{Cl} - 3\text{CO}]^-$, 100), 1534 ($[\text{M} + \text{Cl} - 4\text{CO}]^-$, 85), 1478 ($[\text{M} + \text{Cl} - 6\text{CO}]^-$, 36), 1450 ($[\text{M} + \text{Cl} - 7\text{CO}]^-$, 81).

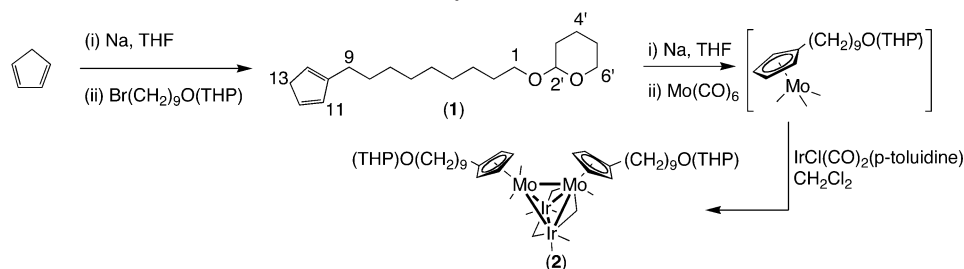
Synthesis of $\text{Mo}_2\text{Ir}_2\{\mu_4\text{-}\eta^2\text{-C}_2[(\text{CH}_2)_6\text{OC(O)NH(CH}_2)_3\text{Me}]_2\}(\mu\text{-CO})_4(\text{CO})_4\{\eta\text{-C}_5\text{H}_5\}_2$ (8**).** Butyl isocyanate (16.0 μL , 142 μmol) and dibutyltin diacetate (DBTA) (4.0 μL , 15 μmol) were added to a solution of cluster **5** (15.4 mg, 13.3 μmol) in THF (5 mL), and the mixture was stirred at room temperature for 24 h. Ethanol (ca. 0.3 mL, 5.5 mmol) was added and the mixture stirred for a further 1 h. All volatiles were removed in vacuo, and the green residue was dissolved in the minimum amount of CH_2Cl_2 and applied to preparative silica TLC plates. Elution with $\text{CH}_2\text{Cl}_2/\text{acetone}$ (9:1) afforded two bands. The contents of the first band (R_f = 0.70, green) were extracted with acetone to afford a green solid, identified as **8** (8.0 mg, 5.9 μmol , 44%). Diffusion of *n*-hexane into a solution of **8** in CH_2Cl_2 at -4°C gave dark green crystals suitable for the structural study. IR: $\nu(\text{CO, cluster})$ 2068 s, 2040 s, 2012 w, 1995 w, 1810 m, 1762 m; $\nu(\text{C=O, urethane})$ 1717 vs; $\delta(\text{N-H})$ 1517 s cm^{-1} . ^1H NMR: δ 4.99 (s, 10H, C_5H_5), 4.65 (br s, 2H, NH), 4.01 (t, J_{HH} = 6.5 Hz, 4H, $\text{CH}_2\text{OC(O)N}$), 3.13 (t, J = 6.3 Hz, 4H, $\text{CH}_2\text{-NHC(O)O}$), 2.11 (m, 4H, CH_2C_2), 1.65–1.22 (m, 24H, CH_2), 0.89 (t, J_{HH} = 7.2 Hz, 6H, CH_3). ^{13}C NMR: δ 96.4 (C_5H_5), 80.2 (C_2), 64.8 ($\text{CH}_2\text{OC(O)N}$), 40.7 ($\text{CH}_2\text{NHC(O)O}$), 32.1, 29.0, 28.5, 25.5, 19.9, 18.7, 13.8. MS (ESI): 1391 ($[\text{M} + \text{Cl}]^-$, 86), 1279 ($[\text{M} + \text{Cl} - 4\text{CO}]^-$, 72), 1251 ($[\text{M} + \text{Cl} - 5\text{CO}]^-$, 100), 1223 ($[\text{M} + \text{Cl} - 6\text{CO}]^-$, 49). Anal. Calcd for $\text{C}_{42}\text{H}_{54}\text{Ir}_2\text{Mo}_2\text{N}_2\text{O}_{12}$: C, 37.22; H, 4.02; N, 2.07. Found: C, 37.92; H, 4.29; N, 1.89. The contents of the second band (R_f = 0.34, green) appeared to be in trace amounts and were not isolated.

Synthesis of $\text{Mo}_2\text{Ir}_2\{\mu_4\text{-}\eta^2\text{-C}_2[(\text{CH}_2)_6\text{OC(O)NH(CH}_2)_3\text{Me}]_2\}(\mu\text{-CO})_4(\text{CO})_4\{\eta\text{-C}_5\text{H}_4\text{Me}\}_2$ (9**).** Butyl isocyanate (30.0 μL , 266 μmol) and DBTA (4.0 μL , 15 μmol) were added to a solution of

cluster **6** (24.5 mg, 20.7 μmol) in *p*-dioxane (5 mL), and the mixture was stirred at room temperature for 24 h. Ethanol (ca. 0.3 mL, 5.5 mmol) was added and the mixture stirred for a further 1 h. All volatiles were removed in vacuo, and the green residue was dissolved in the minimum amount of CH_2Cl_2 and applied to preparative silica TLC plates. Elution with $\text{CH}_2\text{Cl}_2/\text{acetone}$ (9:1) afforded 2 bands. The contents of the first band (R_f = 0.82, green) were extracted with acetone to afford a green solid, identified as **9** (18.8 mg, 13.6 μmol , 66%). Diffusion of *n*-hexane into a solution of **9** in CH_2Cl_2 at -4°C gave dark green crystals. IR: $\nu(\text{CO, cluster})$ 2065 s, 2037 s, 2009 w, 1992 w, 1810 m, 1762 m; $\nu(\text{C=O, urethane})$ 1717 vs; $\delta(\text{N-H})$ 1517 s cm^{-1} . ^1H NMR: δ 4.77–4.67 (m, 10H, $\text{C}_5\text{H}_4 + \text{NH}$), 4.02 (t, J_{HH} = 6.5 Hz, 4H, $\text{CH}_2\text{OC(O)N}$), 3.12 (t, J_{HH} = 6.3 Hz, 4H, $\text{CH}_2\text{NHC(O)O}$), 2.10 (m, 4H, CH_2C_2), 1.59–1.17 (m, 24H, CH_2), 0.88 (t, J_{HH} = 7.2 Hz, 6H, CH_3). ^{13}C NMR (CDCl_3): δ 103.6 ($\text{C}_5\text{H}_4\text{Me}$), 98.5 ($\text{C}_5\text{H}_4\text{Me}$), 95.9 ($\text{C}_5\text{H}_4\text{Me}$), 80.2 (C_2), 64.8 ($\text{CH}_2\text{OC(O)N}$), 40.7 ($\text{CH}_2\text{NHC(O)O}$), 32.1, 29.0, 28.5, 26.0, 25.5, 19.9, 18.7, 13.8. HR-MS (ESI): 1419 ($[\text{M} + \text{Cl}]^-$, 65), 1307 ($[\text{M} + \text{Cl} - 4\text{CO}]^-$, 50). Anal. Calcd for $\text{C}_{44}\text{H}_{59}\text{Ir}_2\text{Mo}_2\text{N}_2\text{O}_{12}$: C, 38.21; H, 4.23; N, 2.03. Found: C, 38.49; H, 4.47; N, 2.23. The contents of the second band (R_f = 0.43, green) were extracted with acetone and taken to dryness on a rotary evaporator to give a green solid, identified as $\text{Mo}_2\text{Ir}_2\{\mu_4\text{-}\eta^2\text{-C}_2[(\text{CH}_2)_6\text{OC(O)NH(CH}_2)_3\text{Me}][(\text{CH}_2)_6\text{OH}]\}(\mu\text{-CO})_4(\text{CO})_4\{\eta\text{-C}_5\text{H}_4\text{Me}\}_2$ (**10**) (3.7 mg, 2.9 μmol , 14%). IR: $\nu(\text{CO, cluster})$ 2065 s, 2037 s, 2008 w, 1992 w, 1810 m, 1761 m; $\nu(\text{C=O, urethane})$ 1716 vs; $\delta(\text{N-H})$ 1516 s cm^{-1} . ^1H NMR: δ 4.77–4.64 (m, 10H, $\text{C}_5\text{H}_4\text{Me} + \text{NH}$), 4.01 (t, J_{HH} = 6.6 Hz, 2H, $\text{CH}_2\text{OC(O)N}$), 3.62 (t, J_{HH} = 6.6 Hz, 2H, CH_2OH), 3.13 (t, J_{HH} = 6.3 Hz, 2H, $\text{CH}_2\text{-NHC(O)O}$), 2.12 (m, 4H, CH_2C_2), 1.60–1.22 (m, 20H, CH_2), 0.89 (t, J_{HH} = 7.2 Hz, 6H, CH_3). MS (ESI): 1320 ($[\text{M} + \text{Cl}]^-$, 45), 1208 ($[\text{M} + \text{Cl} - 4\text{CO}]^-$, 70). Insufficient material precluded microanalysis.

Synthesis of $\text{Mo}_2\text{Ir}_2\{\mu_4\text{-}\eta^2\text{-C}_2[(\text{CH}_2)_6\text{OC(O)NH(CH}_2)_3\text{Me}]_2\}(\mu\text{-CO})_4(\text{CO})_4\{\eta\text{-C}_5\text{H}_4(\text{CH}_2)_9\text{O(THP)}\}_2$ (11**).** Butyl isocyanate (10.0 μL , 88.8 μmol) and DBTA (4.0 μL , 15 μmol) were added to a solution of cluster **7** (9.0 mg, 5.6 μmol) in *p*-dioxane (5 mL), and the mixture was stirred at room temperature for 24 h. Ethanol (ca. 0.3 mL, 5.5 mmol) was added and the mixture stirred for a further 1 h. All volatiles were removed in vacuo, and the green residue was dissolved in the minimum amount of CH_2Cl_2 and applied to preparative silica TLC plates. Elution with $\text{CH}_2\text{Cl}_2/\text{acetone}$ (9:1) afforded 2 bands: The contents of the first band (R_f = 0.78, green) were extracted with acetone to afford a green oil, identified as **11** (2.4 mg, 1.3 μmol , 24%). IR: $\nu(\text{CO, cluster})$ 2065 vs, 2037 vs, 2009 m, 1992 m, 1811 s, 1762 m; $\nu(\text{C=O, urethane})$ 1717 s; $\delta(\text{N-H})$ 1517 m cm^{-1} . ^1H NMR: δ 4.83–4.80 (m, 8H, $\text{C}_5\text{H}_4\text{R}$), 4.62–4.53 (m, 4H, $\text{H}_2' + \text{NH}$), 4.04–4.01 (m, 4H, $\text{CH}_2\text{-OC(O)N}$), 3.87–3.81 and 3.50–3.43 (2 m, 4H, H_6'), 3.73–3.59 and 3.39–3.31 (2 m, 4H, $\text{CH}_2\text{O(THP)}$), 3.16–3.12 (m, 4H, $\text{CH}_2\text{-NHC(O)O}$), 2.29–2.23 (m, 4H, $\text{CH}_2\text{C}_5\text{H}_4$), 2.14–2.09 (m, 4H, CH_2C_2), 1.58–1.20 (m, 64H, CH_2), 0.91–0.85 (m, 6H, CH_3). The contents of the second band (R_f = 0.72, green) appeared to be in trace amounts and were not isolated.

Synthesis of Polyurethane $[-\text{O}(\text{CH}_2)_6(\mu_4\text{-}\eta^2\text{-C}_2)\{\text{Mo}_2\text{Ir}_2(\mu\text{-CO})_4(\text{CO})_4\{\eta\text{-C}_5\text{H}_4\text{Me}\}_2\}(\text{CH}_2)_6\text{OC(O)NH(CH}_2)_4\text{NHC(O)-}]_n$ (12**).** 1,4-Diisocyanatobutane in *p*-dioxane (8.80 mL, 7.88 mM, 69.3 μmol) and DBTA (8.0 μL , 30 μmol) were added to a solution of cluster **6** (77.7 mg, 65.6 μmol) in *p*-dioxane (2 mL), and the mixture was stirred at 40°C for 72 h. Ethanol (ca. 0.5 mL, 9.0 mmol) was added and the mixture stirred for a further 1 h at 40°C . After the reaction had cooled to room temperature, all volatile materials were removed in vacuo. The residue was dissolved in THF (ca. 5 mL) and filtered into a vial. A layer of *n*-hexane was carefully added to the crude oligomer solution, and the two layers were allowed to diffuse at 4°C over 48 h. The mother liquor was decanted from the precipitate, and the diffusion/precipitation process was repeated with chloroform and *n*-hexane. Removal of the supernatant and drying in vacuo yielded the polymer **12** as a waxy green solid (43.4 mg, 56%). IR: $\nu(\text{CO, cluster})$ 2065 vs, 2037 vs, 2014 m, 1992 m, 1809 m, 1762 m; $\nu(\text{C=O, urethane})$ 1711 s; $\delta(\text{N-H})$ 1518 w cm^{-1} .

Scheme 1. Syntheses of **1** and **2**

^1H NMR: δ 4.79–4.68 (m, $\text{C}_5\text{H}_4\text{Me}$), 4.05–3.98 (m, $\text{CH}_2\text{OC}(\text{O})\text{N}$), 3.21–3.09 (m, $\text{CH}_2\text{NHC}(\text{O})\text{O}$), 2.13–2.08 (m, CH_2C_2), 1.76–1.18 (m, CH_2).

Synthesis of polyurethane $[-\text{O}(\text{CH}_2)_6(\mu_4\text{-}\eta^2\text{-C}_2)\{\text{Mo}_2\text{Ir}_2(\mu\text{-CO})_4(\text{CO})_4(\eta\text{-C}_5\text{H}_4(\text{CH}_2)_9\text{OH})_2\}(\text{CH}_2)_6\text{OC}(\text{O})\text{NH}(\text{CH}_2)_4\text{NHC}(\text{O})-]_n$ (**14**). 1,4-Diisocyanatobutane in *p*-dioxane (3.40 mL, 7.88 mM, 26.8 μmol) and DBTA (8.0 μL , 30 μmol) were added to a solution of cluster **7** (43.0 mg, 26.7 μmol) in *p*-dioxane (2 mL), and the mixture was stirred at 40 $^\circ\text{C}$ for 72 h. Ethanol (ca. 0.5 mL, 9.0 mmol) was added and the mixture stirred for a further 1 h at 40 $^\circ\text{C}$. After the reaction cooled to room temperature, all volatile materials were removed in vacuo to afford **13**. IR: $\nu(\text{CO}$, cluster) 2065 vs, 2037 vs, 2012 m, 1992 m, 1811 m, 1762 m; $\nu(\text{C}=\text{O}$, urethane) 1717 vs; $\delta(\text{N}-\text{H})$ 1517 cm^{-1} . The compound was not characterized further but was instead dissolved in ethanol (ca. 15 mL). Pyridinium *p*-toluenesulfonate (PPTS) (10.2 mg, 40.6 μmol) was added and the mixture allowed to stir at 55 $^\circ\text{C}$ for 24 h. All volatile materials were removed in vacuo, and the residue was dissolved in THF (ca. 3 mL). The crude oligomer solution was filtered into a vial and a layer of *n*-hexane was carefully added, and the two layers were allowed to diffuse at 4 $^\circ\text{C}$ over 48 h. The mother liquor was decanted from the precipitate, and the diffusion/precipitation process was repeated with chloroform and *n*-hexane. Removal of the liquid and drying in vacuo yielded the polymer **14** as a waxy green solid (29.4 mg, 68%). IR: $\nu(\text{CO}$, cluster) 2065 vs, 2037 vs, 2012 m, 1992 m, 1810 m, 1762 m; $\nu(\text{C}=\text{O}$, urethane) 1715 vs; $\delta(\text{N}-\text{H})$ 1518 cm^{-1} . ^1H NMR: δ 4.09–3.95 (m, $\text{CH}_2\text{OC}(\text{O})\text{N}$), 3.64–3.57 (m, CH_2OH), 3.36–3.22 (m, $\text{CH}_2\text{NHC}(\text{O})\text{O}$), 2.41–2.28 (m, CH_2C_2), 1.82–1.25 (m, CH_2).

Synthesis of Cross-Linked Polyurethane 15. 1,4-Diisocyanatobutane in *p*-dioxane (1.40 mL, 7.88 mM, 11.0 μmol) and DBTA (8.0 μL , 30 μmol) were added to a solution of polyurethane **14** (19.1 mg, 10.5 μmol) in *p*-dioxane (5 mL), and the mixture was stirred at 40 $^\circ\text{C}$ for 72 h. Ethanol (0.5 mL, 9.0 mmol) was added and the mixture stirred for a further 1 h at 40 $^\circ\text{C}$. After cooling to room temperature, all volatile materials were removed in vacuo. The residue was dissolved in THF (ca. 2 mL) and filtered into a vial. A layer of *n*-hexane was carefully added to the crude oligomer solution, and the two layers were allowed to diffuse at 4 $^\circ\text{C}$ over 48 h. The mother liquor was decanted from the precipitate, and the diffusion/precipitation process was repeated with chloroform and *n*-hexane. Removal of the supernatant and drying in vacuo yielded the polymer **15** as a waxy green solid (11.8 mg, 62%). IR: $\nu(\text{CO}$, cluster) 2065 vs, 2037 vs, 2012 m, 1992 m, 1810 m, 1762 m; $\nu(\text{C}=\text{O}$, urethane) 1715 vs; $\delta(\text{N}-\text{H})$ 1518 cm^{-1} . ^1H NMR: δ 4.04–3.94 (m, $\text{CH}_2\text{OC}(\text{O})\text{N}$), 3.38–3.17 (m, $\text{CH}_2\text{NHC}(\text{O})\text{O}$), 2.37–2.32 (m, CH_2C_2), 1.94–1.23 (m, CH_2).

Synthesis of Polyurethane Copolymer $[-\text{O}(\text{CH}_2)_6(\mu_4\text{-}\eta^2\text{-C}_2)\{\text{Mo}_2\text{Ir}_2(\mu\text{-CO})_4(\text{CO})_4(\eta\text{-C}_5\text{H}_4\text{Me})_2\}(\text{CH}_2)_6\text{OC}(\text{O})\text{NH}(\text{CH}_2)_4\text{NHC}(\text{O})\{\text{O}(\text{CH}_2)_6\text{OC}(\text{O})\text{NH}(\text{CH}_2)_4\text{NHC}(\text{O})\}_m-]_n$ (**16**). To a solution of cluster **6** (93.9 mg, 79.2 μmol , 5%) in *p*-dioxane (10 mL) were added 1,6-hexanediol (175 mg, 1.48 mmol, 95%), 1,4-diisocyanatobutane (0.20 mL, 1.58 mmol), and DBTA (8.0 μL , 30 μmol), and the mixture was stirred at 40 $^\circ\text{C}$ for 72 h. Ethanol (0.5 mL, 9.0 mmol) was added and the mixture stirred for a further 1 h at 40 $^\circ\text{C}$. After the reaction cooled to room temperature, all volatile materials were removed in vacuo. The residue was dissolved in THF (ca. 5 mL) and filtered into a vial. A layer of *n*-hexane was carefully added to the crude oligomer solution, and the two layers

were allowed to diffuse at 4 $^\circ\text{C}$ over 48 h. The mother liquor was decanted from the precipitate, and the diffusion/precipitation process was repeated with chloroform and *n*-hexane. Removal of the supernatant and drying in vacuo yielded the copolymer **16** as a light green solid (56.2 mg, 19%). IR: $\nu(\text{CO}$, cluster) 2065 w, 2037 w; $\nu(\text{C}=\text{O}$, urethane) 1717 vs; $\delta(\text{N}-\text{H})$ 1518 cm^{-1} . ^1H NMR: δ 4.07–3.99 (m, $\text{CH}_2\text{OC}(\text{O})\text{N}$), 3.21–3.11 (m, $\text{CH}_2\text{NHC}(\text{O})\text{O}$), 1.65–1.12 (m, CH_2).

X-ray Crystal Structure Analysis of 5. Crystal data: $\text{C}_{32}\text{H}_{34}\text{Ir}_2\text{Mo}_2\text{O}_{10}\cdot\text{CH}_2\text{Cl}_2$, $M_r = 1239.87$, monoclinic, $P2_1/n$ (No. 14), $a = 9.3573(1)$, $b = 27.8567(3)$, $c = 14.4282(2)$ \AA , $\beta = 98.6340(6)^\circ$, $V = 3718.28(8)$ \AA^3 , $Z = 4$, $\mu = 7.99$ mm^{-1} , $F(000) = 2344$. Crystal size: $0.39 \times 0.21 \times 0.13$ mm. $D_{\text{calc}} = 2.215$ g cm^{-3} , $\theta = 2.9$ – 27.5° , hkl ranges: $-12 \leq h \leq 12$, $-36 \leq k \leq 36$, $-18 \leq l \leq 18$.

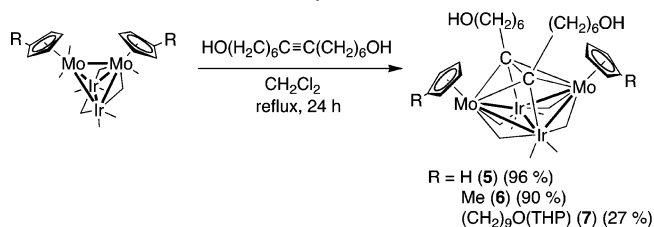
The data were collected at 200 K on a Nonius KappaCCD diffractometer using graphite-monochromated Mo $K\alpha$ radiation ($\lambda = 0.710$ 69 \AA). The unit cell parameters were obtained by least-squares refinement of 80 111 reflections with $2.91 \leq \theta \leq 27.48^\circ$. A numerical absorption correction was applied to the data. Of the 71 602 reflections that were collected, 8519 were unique; equivalent reflections were merged ($R_{\text{int}} = 0.11$). The structure was solved by direct methods.¹² The crystallographic asymmetric unit consists of one molecule of **5** and one molecule of dichloromethane. The non-hydrogen atoms were refined anisotropically, hydrogen atoms were placed in calculated positions, except hydroxyl hydrogens which were located in difference maps and refined positionally. The final cycle of full-matrix least-squares refinement was based on 5530 reflections ($I > 3\sigma(I)$) and 439 variable parameters, and converged with $R = 0.0280$, $R_w = 0.0325$.¹³ A final value for the goodness of fit was 1.08 for the 5530 observed reflections. The largest peaks in the final difference electron density map are located near the Ir atoms.

X-ray Crystal Structure Analysis of 8. Crystal data: $\text{C}_{42}\text{H}_{54}\text{Ir}_2\text{Mo}_2\text{N}_2\text{O}_{12}\cdot 0.5\text{CH}_2\text{Cl}_2\cdot 0.5\text{H}_2\text{O}$, $M_r = 1406.69$, monoclinic, $P2_1/n$ (No. 14), $a = 9.2483(2)$, $b = 14.1908(4)$, $c = 37.5723(10)$ \AA , $\beta = 90.8360(14)^\circ$, $V = 4930.5(2)$ \AA^3 , $Z = 4$, $\mu = 5.99$ mm^{-1} , $F(000) = 2723$. Crystal size: $0.36 \times 0.09 \times 0.07$ mm. $D_{\text{calc}} = 1.895$ g cm^{-3} , $\theta = 2.9$ – 25.1° , hkl ranges: $-11 \leq h \leq 11$, $-16 \leq k \leq 16$, $-44 \leq l \leq 44$.

The data were collected at 200 K on a Nonius KappaCCD diffractometer using graphite-monochromated Mo $K\alpha$ radiation ($\lambda = 0.710$ 69 \AA). The unit cell parameters were obtained by least-squares refinement of 186 350 reflections with $2.91 \leq \theta \leq 25.03^\circ$. A numerical absorption correction was applied to the data. Of the 65 025 reflections which were collected, 8678 were unique; equivalent reflections were merged ($R_{\text{int}} = 0.09$). The structure was solved by direct methods.¹² The crystallographic asymmetric unit consists of one molecule of **8** and partial solvation molecules of dichloromethane and water located at the same site. The non-hydrogen atoms were refined anisotropically; hydrogen atoms were placed in calculated positions (water H atoms were not located). The final cycle of full-matrix least-squares refinement was based on 4103 reflections ($I > 3\sigma(I)$) and 561 variable parameters, and converged with $R = 0.055$, $R_w = 0.045$.¹³ A final value for the goodness of fit was 1.12 for the 4103 observed reflections. The largest peaks in the final difference electron density map are located near the Ir atoms.

Further crystallographic structure solution and refinement details are available in the Supporting Information.

Scheme 2. Syntheses of 5–7



Optical Limiting Studies. Optical limiting behavior of the clusters and cluster-containing oligomers was probed at 523 nm using nanosecond laser pulses. A beam from a frequency-doubled diode-pumped Q-switched Nd:YLF laser (with the repetition rate adjusted to 20–100 Hz) was focused to provide fluences on the order of J cm^{-2} . The Z-scan principle¹⁴ was used to obtain nonlinear absorption data for solutions of compounds placed in 1 mm glass cells and with concentrations adjusted to give approximately 70% transmission. Because the pulse duration was approximately 40 ns, several mechanisms contributed simultaneously to the nonlinear absorption, but for simplicity, we compared the merit of the different compounds by computing the effective nonlinear absorption coefficient β_{eff} . One needs to stress that this parameter is dependent on the pulse duration, and may be much bigger than the true two-photon absorption coefficient, which should be determined with much shorter laser pulses.

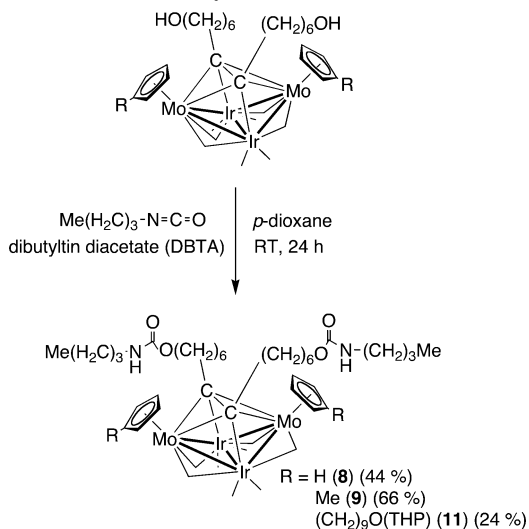
The time-resolved studies of nonlinear absorption used ~50 ps pulses from a laser system comprising a Coherent Antares mode-locked Nd:YLF laser working as an oscillator and a Nd:YLF flashlamp-pumped regenerative amplifier operating at 20 Hz. The output pulses from that system were frequency doubled to provide a 527 nm beam that was split into pump (high intensity) and probe (low intensity) beams. The pump beam was directed through a computer controlled optical delay line before being crossed with the probe beam in the 1 mm glass cell containing the solution under investigation. The transmission of the probe beam was monitored as a function of the relative delay of the pump using a photodiode and a boxcar.

Results and Discussion

Cluster—Diol and —Bis(tetrahydropyranyl) Ether Syntheses. Nucleophilic substitution of bromide in 2-(9-bromononyloxy)tetrahydro-2H-pyran by cyclopentadienide affords the pale yellow liquid 2-(9-(cyclopenta-1,4-dienyl)nonyloxy)-tetrahydro-2H-pyran (**1**) (as a mixture of isomers) in 60% yield (Scheme 1). The tetrahydropyranyl protecting group can be removed at this stage under acidic conditions, but is required for subsequent reactions and so is preserved. Compound **1** was characterized by ¹H NMR and ¹³C NMR spectroscopy and EI mass spectrometry, and its composition was confirmed by high-resolution mass spectrometry. The ¹H NMR spectrum of **1** shows four different sets of multiplets between 3.9 and 3.1 ppm corresponding to the two different hydrogen environments of carbons 1 and 6', while a triplet at 4.56 ppm is assigned to the hydrogen atom of carbon 2'. The protons of carbons 11, 12, and 14 resonate as a multiplet between 6.42 and 5.96 ppm, while the protons of carbon 13 are seen between 2.92 and 2.85 ppm. A multiplet between 2.38 and 2.30 ppm corresponds to the methylene group of C(9). The mass spectrum contains a molecular ion and fragment ions corresponding to loss of the tetrahydropyranyl-protecting group.

η^5 -Cyclopentadienyl and μ_4 - η^2 -alkyne ligands are strongly bound to cluster cores and so were chosen as an appropriate mode of coupling cluster units to the alcohol groups. Compound **1** reacts with sodium in THF to afford the corresponding cyclopentadienide anion, which reacts with Mo(CO)_6 to give the anion $[\text{Mo(CO)}_3\{\eta\text{-C}_5\text{H}_4(\text{CH}_2)_9\text{O(THP)}\}]^-$ (Scheme 1). This

Scheme 3. Syntheses of 8, 9, and 11



functionalized (cyclopentadienyl)molybdenum carbonylate was not isolated, but rather reacted with $\text{IrCl(CO)}_2(p\text{-toluidine})$ to afford cluster **2** as an oil in 28% yield (Scheme 1). The identity of **2** was confirmed by ¹H NMR, ¹³C NMR and IR spectroscopy and high-resolution ESI mass spectrometry. The IR spectrum shows the typical carbonyl stretching frequencies associated with a Mo_2Ir_2 cluster,^{7,8} containing bands corresponding to terminal carbonyls ($2059\text{--}1925\text{ cm}^{-1}$) and bridging carbonyls ($1846\text{--}1758\text{ cm}^{-1}$). The mass spectrum contains a molecular ion plus sodium adduct and a fragment ion corresponding to loss of two carbonyls.

The second type of diol-containing cluster was prepared via the established methodologies for the insertion of alkynes into clusters of the type $\text{M}_2\text{Ir}_2(\text{CO})_{10}(\eta\text{-C}_5\text{H}_4\text{R})_2$ ($\text{M} = \text{Mo}, \text{W}$).^{10,15} Reactions between the clusters $\text{Mo}_2\text{Ir}_2(\mu\text{-CO})_3(\text{CO})_7(\eta\text{-C}_5\text{H}_5)_2$ (**3**), $\text{Mo}_2\text{Ir}_2(\mu\text{-CO})_3(\text{CO})_7(\eta\text{-C}_5\text{H}_4\text{Me})_2$ (**4**), or **2** and tetradec-7-yne-1,14-diol in CH_2Cl_2 yield $\text{Mo}_2\text{Ir}_2\{\mu_4\text{-}\eta^2\text{-C}_2[(\text{CH}_2)_6\text{OH}]_2\}\text{-}(\mu\text{-CO})_4(\text{CO})_4(\eta\text{-C}_5\text{H}_4\text{R})_2$ [$\text{R} = \text{H}$ (**5**), Me (**6**), $(\text{CH}_2)_9\text{O(THP)}$ (**7**)] in moderate to excellent yield as green solids (**5**, **6**) or as a green oil (**7**) (Scheme 2).

The pseudo-octahedral clusters **5**, **6**, and **7** were characterized by ¹H NMR, ¹³C NMR, and IR spectroscopy and high-resolution ESI mass spectrometry. The IR spectra show the typical carbonyl stretching frequencies associated with an alkyne-inserted Mo_2Ir_2 cluster,^{10,15,16} namely four bands in the terminal carbonyl region ($2068\text{--}1991\text{ cm}^{-1}$) and two in the bridging region ($1810\text{--}1759\text{ cm}^{-1}$). The mass spectrum of **6** was obtained in the presence of a small amount of sodium methoxide and contains a strong molecular ion and an OMe adduct. The mass spectra of **5** and **7** and other compounds in the present study were obtained in negative ion mode in the presence of dichloromethane, and they feature chloride adducts of the molecular ion¹⁷ and the typical cluster carbonyl fragmentation by loss of carbonyl groups.

X-ray Study of $\text{Mo}_2\text{Ir}_2\{\mu_4\text{-}\eta^2\text{-C}_2[(\text{CH}_2)_6\text{OH}]_2\}\text{-}(\mu\text{-CO})_4\text{-}(\text{CO})_4(\eta\text{-C}_5\text{H}_5)_2$ (5**).** Figure 2 contains an ORTEP plot of **5** showing the molecular geometry, together with selected bond lengths. Cluster **5** has a Mo_2Ir_2 core in which the metal atoms adopt a butterfly geometry, with the iridium atoms forming the hinge and the molybdenum atoms at the wing tip sites. The alkyne ligand bridges all four metals in a $\mu_4\text{-}\eta^2$ -fashion, lying parallel to the $\text{Ir}(1)\text{--Ir}(2)$ vector, completing a pseudo-octahedral core geometry. The alkyne core carbons interact more strongly with iridium [Ir--C 2.146(5), 2.093(6) Å] than with molybdenum [Mo--C 2.331(5)–2.383(5) Å]. Each molybdenum

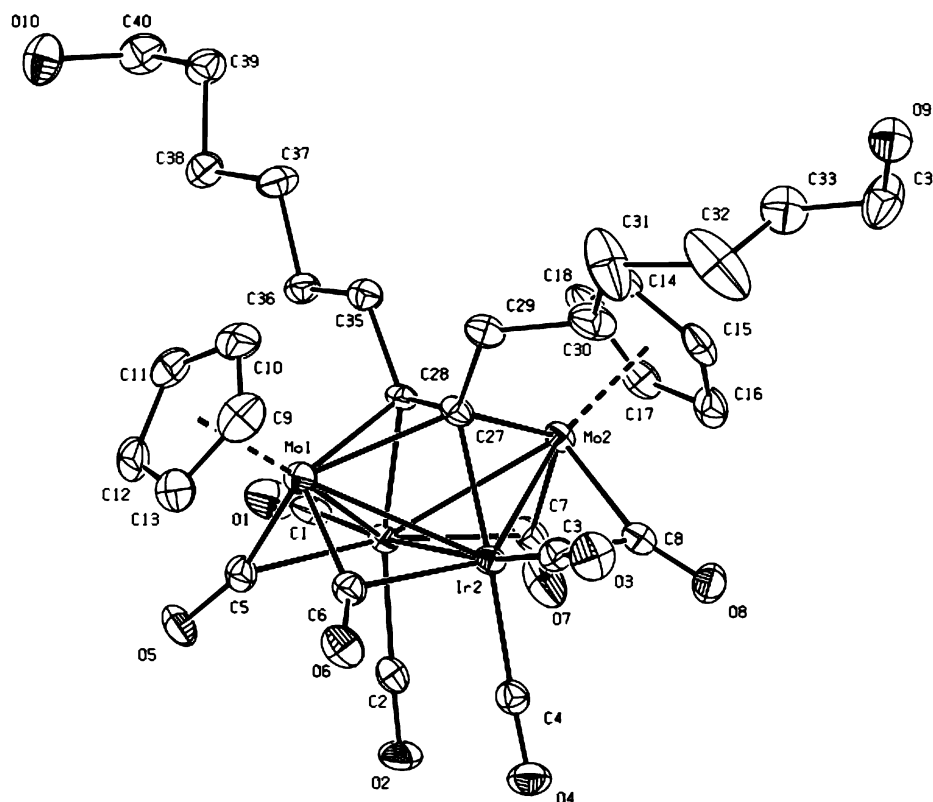


Figure 2. ORTEP plot of $\text{Mo}_2\text{Ir}_2\{\mu_4\text{-}\eta^2\text{-C}_2[(\text{CH}_2)_6\text{OH}]_2\}(\mu\text{-CO})_4(\text{CO})_4(\eta\text{-C}_5\text{H}_5)_2$ (**5**); hydrogens have been omitted for clarity. Selected bond lengths (Å): Ir(1)–Ir(2) 2.7068(5), Ir(1)–Mo(1) 2.7870(7), Ir(1)–Mo(2) 2.7855(7), Ir(2)–Mo(1) 2.8274(7), Ir(2)–Mo(2) 2.8416(8), Ir(1)–C(1) 1.902(6), Ir(1)–C(2) 1.914(6), Ir(2)–C(3) 1.922(6), Ir(2)–C(4) 1.909(6), Ir(1)–C(5) 2.308(6), Ir(1)–C(7) 2.353(6), Ir(2)–C(6) 2.307(6), Ir(2)–C(8) 2.359(6), Mo(1)–C(5) 1.993(6), Mo(1)–C(6) 1.980(6), Mo(2)–C(7) 1.984(6), Mo(2)–C(8) 1.995(6), Ir(1)–C(28) 2.146(5), Ir(2)–C(27) 2.093(6), Mo(1)–C(27) 2.352(6), Mo(1)–C(28) 2.331(5), Mo(2)–C(27) 2.383(5), Mo(2)–C(28) 2.337(5), C(27)–C(28) 1.421(8).

atom bears a cyclopentadienyl ring and each iridium atom is ligated by two terminal carbonyl ligands. All molybdenum–iridium bonds are spanned by a bridging carbonyl ligand, unsymmetrically disposed toward the molybdenum atoms; these carbonyl ligands are borderline semibridging, with asymmetry parameters¹⁸ in the range $\alpha = 0.158\text{--}0.186$. All bond lengths and angles are unexceptional, similar to those of the previously reported analogue.⁴ The lattice packing of **5** shows extensive H-bonding, with four clusters linked in each tetrahydroxy H-bonding motif.

Syntheses of Cluster-Containing Oligourethanes. In order to aid the spectroscopic identification of the cluster-containing oligo- and polyurethanes, a number of model diurethanes were prepared. The reactions between the diol clusters **5**, **6**, and **7** and butyl isocyanate in the presence of a catalytic amount of dibutyltin diacetate yield the green complexes $\text{Mo}_2\text{Ir}_2\{\mu_4\text{-}\eta^2\text{-C}_2[(\text{CH}_2)_6\text{OC}(\text{O})\text{NH}(\text{CH}_2)_3\text{Me}]_2\}(\mu\text{-CO})_4(\text{CO})_4(\eta\text{-C}_5\text{H}_4\text{R})_2$ [$\text{R} = \text{H}$ (**8**), Me (**9**), $(\text{CH}_2)_9\text{O}(\text{THP})$ (**11**)] in moderate to good yield (Scheme 3) accompanied, in the case of **9**, by the monourethane cluster $\text{Mo}_2\text{Ir}_2\{\mu_4\text{-}\eta^2\text{-C}_2[(\text{CH}_2)_6\text{OC}(\text{O})\text{NH}(\text{CH}_2)_3\text{Me}][(\text{CH}_2)_6\text{OH}]\}(\mu\text{-CO})_4(\text{CO})_4(\eta\text{-C}_5\text{H}_4\text{Me})_2$ (**10**) in low yield.

The identities of **8**, **9**, and **11** were confirmed by ^1H NMR, ^{13}C NMR, IR spectroscopy and high-resolution ESI mass spectrometry. IR, ^1H NMR, and ^{13}C NMR spectra of the model complexes are almost identical to those of their precursors, the notable exceptions being the downfield shift of the alkoxy methylene resonance from 3.62 to 4.01 ppm, and the appearance of two triplets at 3.12 and 0.88 ppm corresponding to the methylene group adjacent to the nitrogen atom and the methyl group of the urethane, respectively.

X-ray Study of $\text{Mo}_2\text{Ir}_2\{\mu_4\text{-}\eta^2\text{-C}_2[(\text{CH}_2)_6\text{OC}(\text{O})\text{NH}(\text{CH}_2)_3\text{Me}]_2\}(\mu\text{-CO})_4(\text{CO})_4(\eta\text{-C}_5\text{H}_5)_2$ (8**).** Figure 3 contains an ORTEP plot of **8** showing the molecular geometry, together with selected bond lengths. All bond lengths and angles are unexceptional and similar to those of the previously reported analogue.⁴ As is the case with **5**, the lattice packing of **8** shows extensive H-bonding, with infinite planes resulting from $\text{N}\cdots\text{H}\cdots\text{OC}$ interactions.

Syntheses of Cluster-Containing Oligo- and Polyurethanes. The oligourethanes $[-\text{O}(\text{CH}_2)_6(\mu_4\text{-}\eta^2\text{-C}_2)\{\text{Mo}_2\text{Ir}_2(\mu\text{-CO})_4(\text{CO})_4(\eta\text{-C}_5\text{H}_4\text{R})_2\}(\text{CH}_2)_6\text{OC}(\text{O})\text{NH}(\text{CH}_2)_4\text{NHC}(\text{O})-]_n$ [$\text{R} = \text{Me}$ (**12**), $(\text{CH}_2)_9\text{O}(\text{THP})$ (**13**)] were synthesized from **6** and **7**, respectively (Scheme 4). The syntheses of the oligourethanes were found to proceed best when the cluster precursors were reacted with equimolar amounts of 1,4-diisocyanatobutane in *p*-dioxane at 40 °C for 3 days in the presence of a catalytic amount of dibutyltin diacetate. Reactions in which the solvent was THF, or the reaction times were shorter, yielded dimers at best, and reactions in which the temperature was increased resulted in decomposition. IR (**12**, **13**) and ^1H NMR (**12**) spectroscopy of the oligomers were identical to those of their model complexes **9** and **11**, apart from broadening of the oligomer ^1H NMR resonances. Differential scanning calorimetry studies of **12** reveal that it undergoes a glass transition at ca. 40 °C and decomposes at ca. 250 °C, typical for a polyurethane.

Removal of the tetrahydropyranyl protecting groups from polymer **13** is achieved by dissolving the polymer in ethanol with pyridinium *p*-toluenesulfonate (PPTS) affording $[-\text{O}(\text{CH}_2)_6(\mu_4\text{-}\eta^2\text{-C}_2)\{\text{Mo}_2\text{Ir}_2(\mu\text{-CO})_4(\text{CO})_4(\eta\text{-C}_5\text{H}_4(\text{CH}_2)_9\text{OH})_2\}(\text{CH}_2)_6\text{OC}(\text{O})\text{NH}(\text{CH}_2)_4\text{NHC}(\text{O})-]_n$ (**14**), subsequent cross-polymerization of the unmasked functionalized cyclopentadienyl ring giving

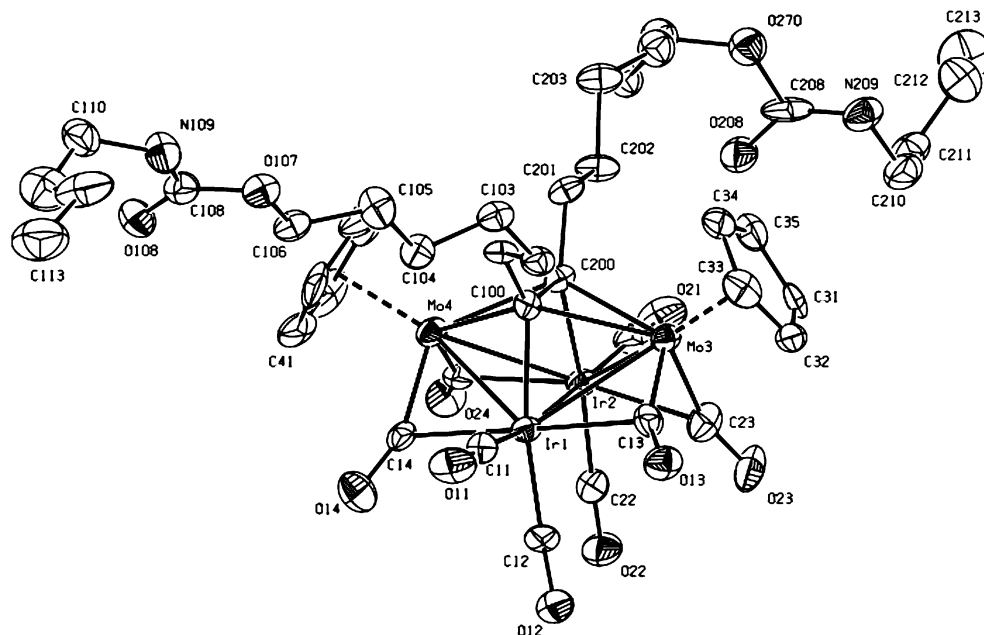
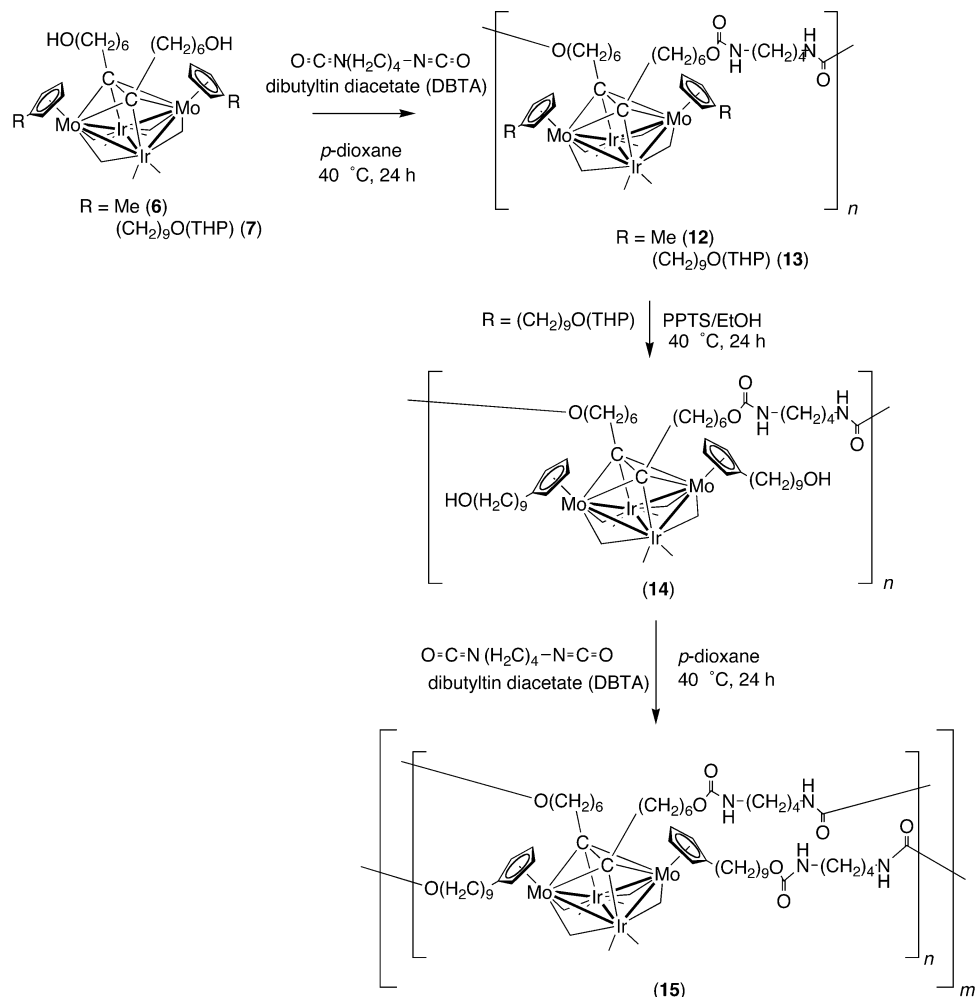


Figure 3. ORTEP plot of $\text{Mo}_2\text{Ir}_2\{\mu_4\text{-}\eta^2\text{-C}_2[(\text{CH}_2)_6\text{OC(O)NH}(\text{CH}_2)_3\text{Me}]_2\}(\mu\text{-CO})_4(\text{CO})_4(\eta\text{-C}_5\text{H}_5)_2$ (**8**); hydrogens have been omitted for clarity. Selected bond lengths (Å): Ir(1)–Ir(2) 2.7166(13), Ir(1)–Mo(1) 2.814(2), Ir(1)–Mo(2) 2.827(2), Ir(2)–Mo(1) 2.788(2), Ir(2)–Mo(2) 2.778(2), Ir(1)–C(1) 1.87(3), Ir(1)–C(2) 1.91(2), Ir(2)–C(3) 1.80(3), Ir(2)–C(4) 1.91(2), Ir(1)–C(5) 2.31(2), Ir(1)–C(7) 2.43(2), Ir(2)–C(8) 2.43(2), Mo(1)–C(5) 2.01(3), Mo(1)–C(6) 1.94(2), Mo(2)–C(7) 1.95(3), Mo(2)–C(8) 2.00(2), Ir(1)–C(27) 2.091(18), Ir(2)–C(28) 2.122(6), Mo(1)–C(27) 2.360(16), Mo(1)–C(28) 2.329(7), Mo(2)–C(27) 2.379(19), Mo(2)–C(28) 2.361(7), C(27)–C(28) 1.436(19).

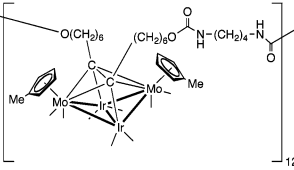
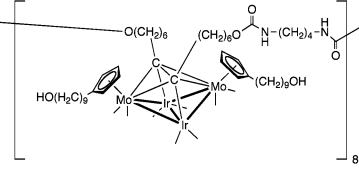
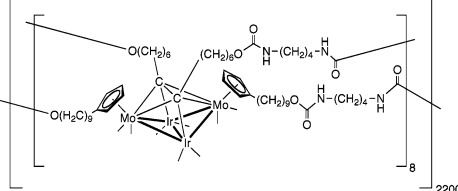
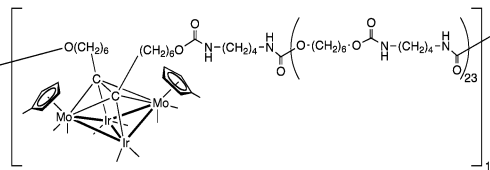
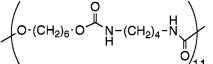
Scheme 4. Syntheses of Polymers 12–15



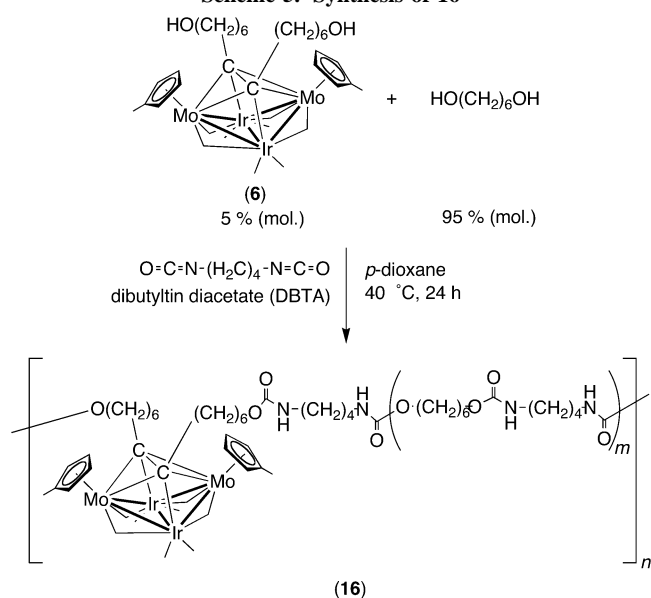
15 (Scheme 4). IR and ^1H NMR spectra of **15** are similar to those of the model complex **11**, and show the disappearance of

the protons of the protecting group; the ^1H NMR resonances are broadened, as expected.

Table 1. Estimated Molecular Weight Averages for Cluster Polymers 12 and 14–16

Compound	Molecular weight of repeat unit	Estimated molecular weight from calibration curve	Average number of repeat units	Polydispersity
12	1325	1.62×10^4		3.13
14	1582	1.19×10^4		1.69
15	11900	2.70×10^7		1.14
16 (peak 1)	1325 (cluster) 258 (organic)	7.20×10^3		1.15
16 (peak 2)	1325 (cluster) 258 (organic)	2.80×10^3		1.03

Scheme 5. Synthesis of 16

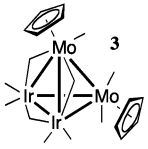
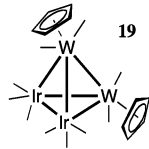
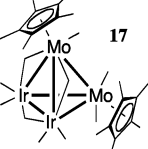
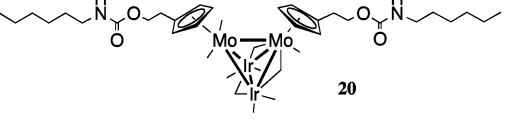
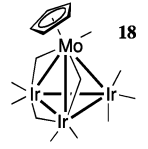
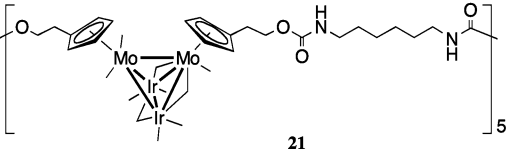
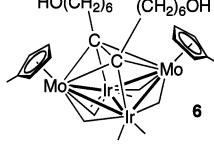
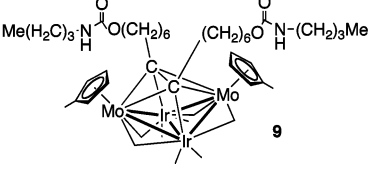


The cluster content of the polymers may be diluted by use of a second organic diol monomer. The reaction of 5 mol % of

6 and 95 mol % of 1,6-hexanediol with 1,4-diisocyanatobutane affords the copolymer $[-O(CH_2)_6(\mu_4-\eta^2-C_2)\{Mo_2Ir_2(\mu-CO)_4-(CO)_4(\eta-C_5H_4Me)_2\}(CH_2)_6OC(O)NH(CH_2)_4NHC(O)\{O(CH_2)_6-OC(O)NH(CH_2)_4NHC(O)\}_m-]_n$ (16) (Scheme 5). IR and 1H NMR spectra of 16 are as expected, being similar to those of the model complex 9, but with broadening of the 1H NMR resonances.

The extent of polymerization was assessed by size exclusion chromatography (SEC). SEC of the well-defined model complex 9 (calibrated against polystyrene standards) gave a molecular weight significantly lower than that expected, so a number of similar, well-defined complexes were subjected to SEC under identical conditions in order to construct a calibration curve. The calibration curve of known molecular weight cluster-containing species vs retention time on the column gave a good fit for a linear regression line, and so this, along with integration of 1H NMR resonances of terminal and bridging methylene groups, was used in order to approximate the extent of polymerization of the polymers, the results of which are listed in Table 1. All polymers contained a single maximum in their SEC trace, with the exception of copolymer 16, which contained two maxima; with 16, the first maximum corresponds to one part cluster unit to 23 parts organic units, and the second maximum corresponds to an organic oligomer with 11 repeat

Table 2. Optical Limiting Results Derived from Open-Aperture Z-Scan Experiments in CH₂Cl₂ Solutions

β_{eff} (10 ⁻⁶ cm/W) ^a	β_{eff} (10 ⁻⁶ cm/W) ^a
 3	 19
56	74
 17	 20
42	38
 18	 21
24	48
 6	 9
15	15

^a ±20%.

units. The polydispersity of **12** is much higher than that of all the other polymers, but this is attributed to the fact that equimolar ratios were not achieved. The validity of the calibration curve at higher molecular weights is unknown, because the extent of polymerization of **15** is much greater than any of the other polymers. Polymerization of **15** occurs via the functionalized cyclopentadienyl group, compared with polymerization via the alkyne unit of the other polymers, which may account for some difference in the extent of polymerization; further studies are required to substantiate this trend.

Optical Limiting Studies. Linear optical spectra of some examples of the clusters and cluster oligomers above, as well as the related clusters and cluster oligomer **17–21** (see Table 2 for molecular structures), were obtained; all of these species possess broad low intensity absorptions through the visible region, which suggests that they have potential as broadband optical limiters. Incorporation of the cluster into the oligomer (proceeding from **20** to **21**) does not result in modification of the linear optical spectrum, consistent with electronically “insulated” clusters, as expected, permitting optical properties of the cluster to be exploited while processability is enhanced.

The optical power limiting merit of these species was investigated using open-aperture Z-scan measurements. Typical results as well as theoretical curves for a tetrahedral cluster and alkyne adduct [those of Mo₂Ir₂(μ-CO)₃(CO)₇(η-C₅Me₅)₂ (**17**) and Mo₂Ir₂{μ₄-η²-C₂[(CH₂)₆OC(O)NH(CH₂)₃Me]₂}(μ-CO)₄(CO)₄(η-C₅H₄Me)₂ (**9**)] are shown in Figure 4. Nonlinear absorption of **3**, **6**, **9**, and **17–21** are presented in Table 2 as the effective nonlinear absorption coefficients of the pure substances, β_{eff} .

Several trends in β_{eff} are revealed by this study (while being mindful of the error margins). The molybdenum–triiridium cluster **18** exhibits a lower nonlinear absorption coefficient than the dimolybdenum–diiridium cluster **3**, and alkylation of the

cyclopentadienyl ring reduces merit (cf. **3** and **17**), although the effect is less significant. Metal substitution within the same group (e.g., tungsten for molybdenum) results in a sizable increase in β_{eff} for the heavier tungsten-containing analogue **19** compared to **3**. The pseudo-octahedral alkyne-insertion clusters **6** and **9** have lower nonlinear absorption coefficients than the tetrahedral clusters. Proceeding from cluster diol **6** to cluster diurethane **9** does not modify β_{eff} . Similarly, while incorporation of clusters into polymers increases processability, it does not appear to diminish nonlinear absorption, as is seen by comparing the cluster-containing oligomer **21** and model complex **20**. These results are consistent with the optical limiting response originating from the ligated metal core and with no intercluster electronic interaction to influence optical limiting.

Measurements of nonlinear absorption with nanosecond laser pulses are known to give rise to substantial overestimation of two-photon absorption coefficients compared to the values obtained with shorter (femtosecond or picosecond) pulses, due to a number of time-dependent photophysical processes being integrated into the response on the nanosecond time scale.¹⁹ The two-photon absorption (TPA) process is instantaneous and is the most attractive process for providing intensity-dependent transmission. The main advantage of two-photon absorption for optical power limiting is that a two-photon absorber can offer zero or very low absorption at low intensities, but increased absorption at higher intensities to clamp the transmitted power. However, in the case of the clusters investigated in the present study, there is some (weak) one-photon absorption at the wavelength of interest. Proximity of a one-photon absorption peak may be advantageous for increasing the two-photon absorption cross-section through resonant enhancement.²⁰ However, the excited states generated through the one-photon process are also important, since they can provide additional absorption. This effect is called reverse saturable absorption (RSA). Relative contributions of TPA and RSA can be described by writing the

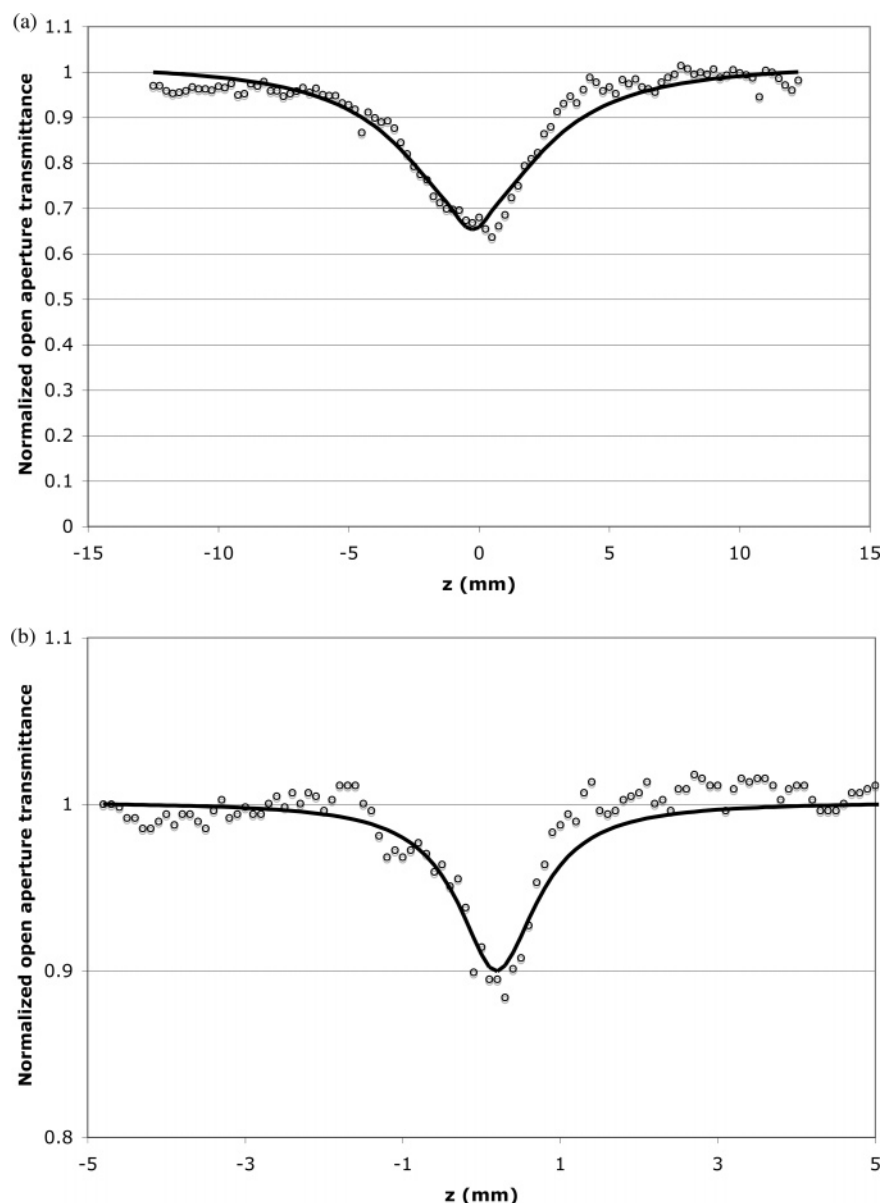


Figure 4. Z-scan data set and ideal fitted curve for (a) $\text{Mo}_2\text{Ir}_2(\mu\text{-CO})_3(\text{CO})_7(\eta\text{-C}_5\text{Me}_5)_2$ (**17**), $w_0 = 35 \mu\text{m}$, $I_{\text{max}} = 126 \text{ MW cm}^{-2}$ and (b) $\text{Mo}_2\text{Ir}_2\{\mu_4\text{-}\eta^2\text{-C}_2[(\text{CH}_2)_6\text{OC}(\text{O})\text{NH}(\text{CH}_2)_3\text{Me}]_2\}(\mu\text{-CO})_4(\text{CO})_4(\eta\text{-C}_5\text{H}_4\text{Me})_2$ (**9**), $w_0 = 11 \mu\text{m}$, $I_{\text{max}} = 82 \text{ MW cm}^{-2}$.

nonlinear Lambert–Beer equation as

$$\frac{dI(t,z)}{dz} = -\alpha I(t,z) - \beta_2 [I(t,z)]^2 - (\alpha_e - \alpha) \frac{N_e(t,z)}{N} I(t,z) \quad (1)$$

where $I(t,z)$ is the light intensity, α is the absorption coefficient, β_2 is the two-photon absorption coefficient, α_e is the excited-state absorption coefficient, N_e denotes the concentration of excited-state chromophore molecules, and N is the total concentration of the chromophores. The three terms on the right-hand side of the above equation denote the one-photon absorption, the two-photon absorption, and the incremental excited-state absorption. Assuming that the population of excited states N_e is generated mostly by one-photon absorption, one can write

$$\frac{dN_e(t,z)}{dt} = \frac{\alpha I(t,z)}{h\nu} \frac{(N - N_e(t,z))}{N} - \frac{N_e(t,z)}{\tau_e} \quad (2)$$

where $h\nu$ is the photon energy and τ_e is the excited-state lifetime.

Integrating the above for long-lived excitations and assuming $N_e \ll N$, a laser pulse having the duration $t_p \ll \tau_e$ will generate

a concentration of excited states which is (taking the average intensity and average concentration):

$$N_e \approx \frac{\alpha I}{h\nu} t_p \quad (3)$$

Inserting this expression into eq 1 and combining the two terms that are quadratic in light intensity, we see that an averaged effective two-photon absorption coefficient β_{eff} can be defined as

$$\frac{dI(z)}{dz} = -\alpha I(z) - \beta_2 [I(z)]^2 - (\alpha_e - \alpha) \frac{\alpha t_p}{N h\nu} [I(z)]^2 = -\alpha I(z) - \beta_{\text{eff}} [I(z)]^2 \quad (4)$$

in which the contribution of the RSA term scales with the laser pulse duration.

To obtain some insight into these issues, we performed a time-resolved pump–probe experiment using relatively short (50 ps) pulses. Pump–probe experiments allow one to determine both the absolute magnitude of the nonlinear absorption and its

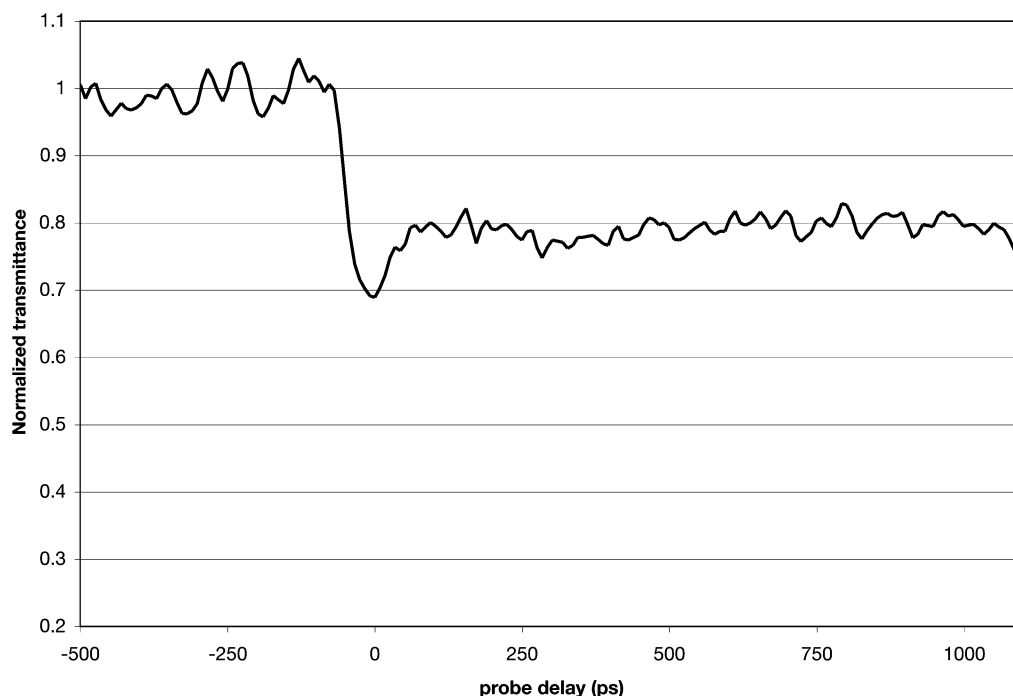


Figure 5. Results from a 527 nm picosecond pump–probe experiment on **22**.

evolution with time and thus give information on lifetimes of states that may be involved in the nonlinear absorption process. These experiments were carried out on examples of a tetrahedral mixed group 6-iridium cluster compound and a pseudo-octahedral alkyne adduct, in order to determine whether these clusters exhibit instantaneous two-photon absorption (TPA) and/or reverse saturable absorption (RSA), the two most desirable mechanisms for optical power limiting. While no signal could be observed for the tetrahedral cluster **7** under our experimental conditions, the alkyne adduct $\text{Mo}_2\text{Ir}_2(\mu_4\text{-}\eta^2\text{-MeC}_5\text{H}_4\text{Ph})(\mu\text{-CO})_4(\text{CO})_4(\eta\text{-C}_5\text{H}_4\text{Me})_2$ (**22**) was sufficiently active, the results from a 527 nm pump–probe experiment (pulses of ca. 50 ps duration, pump fluence at the sample ca. 1 J cm^{-2}) being shown in Figure 5.

Negative delays in the figure correspond to the probe beam arriving at the sample before the pump, and thus the signal at delay < 0 is the background. There is a distinct negative peak at 0 ps (the probe arriving simultaneously with the pump) which has a width corresponding roughly to that of the pulse duration, and thus it is likely to arise from an instantaneous TPA phenomenon involving one photon each from the pump and probe beams. For positive probe delays (the probe beam arrives *after* the pump beam), there is a long-lived tail which is likely to be the result of excited-state absorption of the probe by the metastable states formed by the pump (the RSA process). It can be seen from the tail behavior that the state(s) giving rise to the excited-state absorption are characterized by a long lifetime (definitely > 1000 ps). Compound **22** can thus be classed as an optical power limiter exhibiting both TPA and RSA. The results shown in Figure 5 can be used to estimate the contribution of the two mechanisms to the power limiting in the nanosecond regime. The negative peak at delay = 0 ps has an amplitude that corresponds to the nonlinear absorption coefficient $\beta_2 \approx 10^{-7} \text{ cm W}^{-1}$. With 50 ps pulses the amplitude of the RSA effect appears to be of similar magnitude as that of the TPA effect. However, as explained above, with longer pulses one can expect that the efficiency of the RSA will scale with the pulse duration as long as the pulse duration is shorter than the lifetime of the metastable state. Thus, power limiting with

nanosecond pulses should be characterized by an effective nonlinear absorption coefficient up to 3 orders of magnitude larger than that for 50 ps pulses. This would lead to $\beta_{\text{eff}} \approx 10^{-4} \text{ cm W}^{-1}$, which indeed rationalizes the values of the order of 10^{-5} – $10^{-4} \text{ cm W}^{-1}$ given in Table 2.

Conclusion

The present research has yielded a number of cluster-containing oligomers with the cluster units incorporated into the backbone of the polymer, these polymers being in a form suitable for optical limiting applications. In principle, incorporation of metal clusters into the main-chain of oligourethanes can proceed in one of two ways, either from reactions between a cluster diol and a diisocyanate, or from reactions between a cluster diisocyanate and a diol. The present studies utilized reactions with a cluster diol, as reactions requiring synthetic manipulations of hydrolytically sensitive intermediates are required to prepare cluster diisocyanates. η -Cyclopentadienyl and $\mu_4\text{-}\eta^2$ -alkyne ligands are strongly bound to cluster cores and so were chosen as an appropriate mode of attachment for the alcohol groups. The synthesis of metal cluster units was achieved by extending the pre-existing chemistry for the insertion of alkynes into clusters of the type $\text{Mo}_2\text{Ir}_2(\mu\text{-CO})_3(\text{CO})_7(\eta\text{-C}_5\text{H}_4\text{R})_2$ to embrace an appropriately functionalized alkyne. By simultaneously employing a functionalized cyclopentadienyl ring [$\text{R} = (\text{CH}_2)_9\text{OH}$], this has also afforded a cross-linked polymer of much higher molecular weight.

The cluster-containing materials exhibit optical limiting properties. Open-aperture Z-scan studies have enabled the performance of these systematically varied compounds to be evaluated, affording structure–property trends that identify the key molecular components influencing optical limiting merit. In one case, a pump–probe study has revealed that these materials have a broad temporal optical limiting response, with both two-photon absorption and excited-state absorption behavior being identified.

Acknowledgment. We thank the Australian Research Council for support of this work and Johnson-Matthey Technology

Centre for the generous loan of iridium salts. Prof. R. G. Gilbert and Dr. R. Mahidasht (University of Sydney) are thanked for size exclusion chromatography studies. M.G.H. is an ARC Australian Professorial Fellow, M.P.C. was an ARC Australian Research Fellow, and N.T.L. held an Australian Postgraduate Award.

Supporting Information Available: A cif file giving solution and refinement details and tables of atomic coordinates, bond lengths, and bond angles for the X-ray structural studies of **3** and **6**. This material is available free of charge via the Internet at <http://pubs.acs.org>.

References and Notes

- (1) Part 29: Usher, A. J.; Lucas, N. T.; Dalton, G. T.; Randles, M. D.; Viau, L.; Humphrey, M. G.; Petrie, S.; Stranger, R.; Willis, A. C.; Rae, A. D. *Inorg. Chem.* **2006**, *45*, 10859.
- (2) See, for example: (a) Rafalko, J. J.; Lieto, J.; Gates, B. C.; Schrader, G. L., Jr. *J. Chem. Soc., Chem. Commun.* **1978**, 540. (b) Lieto, J.; Wolf, M.; Matrana, B. A.; Prochazka, M.; Tesche, B.; Knözinger, H.; Gates, B. C. *J. Phys. Chem.* **1985**, *89*, 991. (c) Foster, D. F.; Harrison, J.; Nicholls, B. S.; Smith, A. K. *J. Organomet. Chem.* **1985**, 295, 99. (d) Paetzold, E.; Pracejus, H.; Oehme, G. *J. Mol. Catal.* **1987**, *42*, 301. (e) Bhaduri, S.; Khwaja, H.; Narayanan, B. A. *J. Chem. Soc., Dalton Trans.* **1984**, 2327.
- (3) Dagani, R. *Chem. Eng. News* **1996**, Jan. 1, 24.
- (4) Lucas, N. T.; Humphrey, M. G.; Rae, A. D. *Macromolecules* **2001**, *34*, 6188.
- (5) Klabunde, U. *Inorg. Synth.* **1974**, *15*, 82.
- (6) Churchill, M. R.; Li, Y.-J.; Shapley, J. R.; Foose, D. S.; Uchiyama, W. S. *J. Organomet. Chem.* **1986**, *312*, 121.
- (7) Lucas, N. T.; Humphrey, M. G.; Hockless, D. C. R. *J. Organomet. Chem.* **1997**, *535*, 175.
- (8) Lucas, N. T.; Blitz, J. P.; Petrie, S.; Stranger, R.; Humphrey, M. G.; Heath, G. A.; Otieno-Alego, V. *J. Am. Chem. Soc.* **2002**, *124*, 5139.
- (9) Shapley, J. R.; Hardwick, S. J.; Foose, D. S.; Stucky, G. D. *J. Am. Chem. Soc.* **1981**, *103*, 7383.
- (10) Lucas, N. T.; Notaras, E. G. A.; Cifuentes, M. P.; Humphrey, M. G. *Organometallics* **2003**, *22*, 284.
- (11) Jayasuriya, N.; Bosak, S.; Regen, S. L. *J. Am. Chem. Soc.* **1990**, *112*, 5844.
- (12) Altomare, A.; Cascarano, G.; Giacovazzo, G.; Guagliardi, A.; Burla, M. C.; Polidori, G.; Camalli, M. *J. Appl. Crystallogr.* **1994**, *27*, 435.
- (13) Betteridge, P. W.; Carruthers, J. R.; Cooper, R. I.; Prout, K.; Watkin, D. J. *J. Appl. Crystallogr.* **2003**, *36*, 1487.
- (14) Sheik-Bahae, M.; Said, A. A.; Wei, T.; Hagan, D. J.; van Stryland, E. W. *IEEE J. Quantum Electr.* **1990**, *26*, 760.
- (15) (a) Lucas, N. T.; Notaras, E. G. A.; Petrie, S.; Stranger, R.; Humphrey, M. G. *Organometallics* **2003**, *22*, 708. (b) Notaras, E. G. A.; Lucas, N. T.; Humphrey, M. G.; Willis, A. C.; Rae, A. D. *Organometallics* **2003**, *22*, 3659.
- (16) Lucas, N. T.; Humphrey, M. G.; Healy, P. C.; Williams, M. L. *J. Organomet. Chem.* **1997**, *545–546*, 519.
- (17) Chloride adduct ions from negative ion ESI MS in chlorinated solvents have been reported elsewhere. See, for example: Zhu, J.; Cole, R. B. *J. Am. Soc. Mass Spectrom.* **2000**, *11*, 932.
- (18) (a) Curtis, M. D.; Butler, W. M. *J. Organomet. Chem.* **1978**, *155*, 131. (b) Klingler, R. J.; Butler, W. M.; Curtis, M. D. *J. Am. Chem. Soc.* **1978**, *100*, 5034.
- (19) Rogers, J. E.; Slagle, J. E.; McLean, D. G.; Sutherland, R. L.; Sankaran, B.; Kannan, R.; Tan, L. S.; Fleitz, P. A. *J. Phys. Chem. A* **2004**, *108*, 5514.
- (20) See, for example: (a) Kamada, K.; Ohta, K.; Iwase, Y.; Kondo, K. *Chem. Phys. Lett.* **2003**, *372*, 386. (b) Drobizhev, M.; Stepanenko, Y.; Dzenis, Y.; Karotki, A.; Rebane, A.; Taylor, P. N.; Anderson, H. L. *J. Am. Chem. Soc.* **2004**, *126*, 15352.

MA0710582